IAI Journals.ASM.org

Proteome Analysis of Coinfection of Epithelial Cells with *Filifactor alocis* and *Porphyromonas gingivalis* Shows Modulation of Pathogen and Host Regulatory Pathways

A. Wilson Aruni,[a] Kangling Zhang,[b] Yuetan Dou,[a] Hansel Fletcher[a]

Division of Microbiology and Molecular Genetics, School of Medicine, Loma Linda University, Loma Linda, California, USA[a]; University of Texas Medical Branch at Galveston, Galveston, Texas, USA[b]

Changes in periodontal status are associated with shifts in the composition of the bacterial community in the periodontal pocket. The relative abundances of several newly recognized microbial species, including *Filifactor alocis*, as-yet-unculturable organisms, and other fastidious organisms have raised questions on their impact on disease development. We have previously reported that the virulence attributes of *F. alocis* are enhanced in coculture with *Porphyromonas gingivalis*. We have evaluated the proteome of host cells and *F. alocis* during a polymicrobial infection. Coinfection of epithelial cells with *F. alocis* and *P. gingivalis* strains showed approximately 20% to 30% more proteins than a monoinfection. Unlike *F. alocis* ATCC 35896, the D-62D strain expressed more proteins during coculture with *P. gingivalis* W83 than with *P. gingivalis* 33277. Proteins designated microbial surface component-recognizing adhesion matrix molecules (MSCRAMMs) and cell wall anchor proteins were highly upregulated during the polymicrobial infection. Ultrastructural analysis of the epithelial cells showed formation of membrane microdomains only during coinfection. The proteome profile of epithelial cells showed proteins related to cytoskeletal organization and gene expression and epigenetic modification to be in high abundance. Modulation of proteins involved in apoptotic and cell signaling pathways was noted during coinfection. The enhanced virulence potential of *F. alocis* may be related to the differential expression levels of several putative virulence factors and their effects on specific host cell pathways.

While recent attention has focused on the study of the composition of the human microbiome, the inherent mechanisms underlying the complex interpathogen and host-pathogen interactions leading to polymicrobial infectious diseases of an inflammatory nature are still poorly defined. One such inflammatory disease, periodontitis, has a multifactorial etiology which is influenced by host genetics and several environmental factors. Further, there is evidence that this inflammatory disease affecting the periodontium represents an increased risk for several systemic diseases, including atherosclerosis (1), diabetes (2), and rheumatoid arthritis (3, 4). Historically, periodontal disease is associated with several pathogens contributing to a complex microbial milieu which can initiate or directly contribute to host tissue destruction (5). Bacteria such as *Porphyromonas gingivalis*, *Prevotella intermedia*, *Aggregatibacter* (*Actinobacillus*) *actinomycetemcomitans*, *Tannerella forsythia*, and *Treponema denticola* have previously been demonstrated to be major pathogens associated with periodontal diseases (6–8). A comparative oral microbiome analysis of the healthy and diseased states has indicated diversity in the microbial communities (9, 10). Collectively, these studies have demonstrated that changes in the periodontal status are associated with shifts in the composition of the bacterial community in the periodontal pocket (11, 12). The relative abundances of several newly recognized microbial species, as-yet-unculturable organisms, and other fastidious organisms (9, 13, 14) have raised questions on their impact on disease development.

Filifactor alocis, a Gram-positive, asaccharolytic, obligate anaerobic rod, based on the emerging microbiome data, is one of the marker organisms associated with periodontal inflammation and is suggested to be an important organism for periodontal disease (15–19). Further, in comparison to the other traditional periodontal pathogens, the high incidence of *F. alocis* in the periodontal pocket compared to its absence in healthy or periodontitis-resistant patients could support the idea of its importance in the infectious state of the disease (16, 17, 20). This organism, first isolated in 1985 from the gingival sulcus in gingivitis and periodontics patients, was originally classified as *Fusobacterium alocis* (21). However, based on phylogenetic analysis using 16S rRNA sequences, it was reclassified in 1999 into the genus *Filifactor* (22).

We have earlier demonstrated that *F. alocis* has virulence properties that may enhance its ability to survive and persist in the periodontal pocket (23). For example, it was relatively resistant to oxidative stress and its stimulated growth under those conditions could be an important attribute (23). As reported elsewhere, others have shown that *F. alocis* can induce secretion of proinflammatory cytokines, including interleukin-1β (IL-1β), IL-6, and tumor necrosis factor alpha (TNF-α), from gingival epithelial cells and can trigger apoptosis of these cells (24). Colonization and survival of *F. alocis* in a mouse model showed proapoptotic local infection that was rapidly resolved by host neutrophil influx (25). A comparative analysis of several *F. alocis* isolates showed heterogeneity in their levels of virulence potential (23). *F. alocis* can interact with other important periodontal pathogens such as *P.*

Received 19 March 2014 **Accepted** 15 May 2014
Published ahead of print 27 May 2014
Editor: S. R. Blanke
Address correspondence to Hansel Fletcher, hfletcher@llu.edu.
Supplemental material for this article may be found at http://dx.doi.org/10.1128/IAI.01727-14.

doi:10.1128/IAI.01727-14

gingivalis (26). Further, in coculture with *P. gingivalis*, these *F. alocis* strains showed variations in their capacity for invasion of epithelial cells (23) While synergistic interactions during polymicrobial infections have resulted in enhanced pathogenesis of periodontopathogens such as *P. gingivalis* (27), whether there is a similar mechanism(s) for *F. alocis* is unclear. It is likely that surface and secretory proteins from *F. alocis* play a role in this process.

Host-pathogen interactions are known to induce significant changes in the transcriptional program of the host cells resulting in the mobilization of genes involved in key processes that mediate the appropriate response. Some of these changes may lead to epigenetic modifications that are associated with a variety of biological processes, including cell differentiation, proliferation, and immunity (28, 29). Successful pathogens have developed novel strategies, including bacterially induced epigenetic deregulation that may affect host cell function to facilitate their survival and persistence. Proteomics analyses have significantly contributed toward a deeper understanding of the molecular mechanisms utilized by several oral pathogens such as *Streptococcus mutans* (30), *Streptococcus oralis* (31), *Fusobacterium nucleatum* (32), and *P. gingivalis* (33–35) during their interaction with the host. In a previous host-pathogen interaction study performed with epithelial cells, we showed proteome variation in *F. alocis* with upregulation of many important bacterial proteins (36) that could potentially trigger direct or indirect epigenetic modifications in the host. Because virulence heterogeneity has been observed in *F. alocis* (23), it is unclear which key host pathways were modulated in this interaction that may lead to the differential host response during the infectious process. In this study, we used shotgun proteomics-based differential protein expression analysis and relative quantification of both *F. alocis* and host proteins to study pathogen-dependent host modulations. We have also used metabolomics to evaluate the changes associated with metabolic pathways and networks that could influence the variation in cell responses during the infectious process.

MATERIALS AND METHODS

Bioinformatics analysis. The DNA and amino acid sequences were aligned using Bioedit (http://www.mbio.ncsu.edu/bioedit/bioedit.html). The phylogenetic relationship between the sequences of these oral pathogens was analyzed using MEGA version 4.0 (37). The signal peptide and potential cleavage sites were predicted using both neural network and hidden Markov model methods (38). Metabolic pathway analysis was carried out using the *Kyoto Encyclopedia of Genes and Genomes* (KEGG) (www.genome.jp/kegg/) (39).

Bacterial strains and growth conditions. *F. alocis* ATCC 35896 was purchased from the American Type Culture Collection (Rockville, MD). *F. alocis* D-62D was a gift from Floyd Dewhirst, the custodian of the Moores' anaerobic microbial collection (The Forsyth Institute, Boston, MA). The identity of the *F. alocis* D-62D strain was confirmed by 16S rRNA gene sequencing (D-62D; GenBank accession no. GU968904). *F. alocis* strains were grown initially in Robertson's bullock heart medium followed by adaptation to brain heart infusion (BHI) broth supplemented with hemin (5 μg/ml), vitamin K (0.5 μg/ml), cysteine (1 μg/ml), and arginine (17.42 μg/ml). *P. gingivalis* strains were grown in BHI broth (Difco) supplemented with hemin (5 μg/ml), vitamin K (0.5 μg/ml), and cysteine (0.1%). Blood agar medium was prepared by the addition of sheep blood (5%) and agar (2%). The bacterial cultures were incubated at 37°C in an anaerobic chamber (Coy Manufacturing) in an atmosphere that included 10% H_2, 10% CO_2, and 80% N_2. Growth rates were determined spectrophotometrically (optical density at 600 nm [OD_{600}]).

Epithelial cell culture. HeLa cells were grown and maintained at a density of 2×10^5 cells/ml in a humid incubator with 5% CO_2 at 37°C in Dulbecco's modified Eagle's medium (DMEM) supplemented with 10% fetal bovine serum, penicillin (100 IU/ml), streptomycin (100 IU/ml), and amphotericin B (2.5 mg/ml) (Invitrogen, Carlsbad, CA). The volume of cells was split into two halves, in fresh prewarmed medium. Confluent stock cultures were trypsinized, adjusted to approximately 5×10^3 cells/ml, seeded (1 ml per well) into 12-well plates (Nunc, Rochester, NY), and further incubated for 48 h to reach semiconfluence (10^5 cells per well).

Coculture of *F. alocis* and *P. gingivalis* and standard antibiotic protection assay. Invasion of epithelial cells was quantified using the standard antibiotic protection assay (40). Briefly, an isolated bacterial colony harvested from a solid agar plate was grown to the exponential phase in BHI broth. The bacterial cells were then centrifuged, washed three times in phosphate-buffered saline (PBS), and adjusted to 10^7 CFU/ml of bacteria in DMEM. The epithelial cell monolayer was washed three times with PBS, infected with bacteria at a multiplicity of infection (MOI) of 1:100 (10^5 epithelial cells), and then incubated at 37°C for 30 and 45 min under 5% CO_2. Nonadherent bacteria were removed by washing with PBS, while cell surface-bound bacteria were killed with metronidazole (200 μg/ml, 60 min). *F. alocis* is sensitive to 100 μg/ml of metronidazole. After removal of the antibiotic, the internalized bacteria were released by osmotic lysis of the epithelial cells in sterile distilled water. Lysates were serially diluted, plated (in duplicate) on BHI agar, and incubated for 6 to 10 days. The number of bacterial cells recovered was expressed as a percentage of the original inoculum. The number of adherent bacteria was obtained by subtracting the number of intracellular bacteria from the total number of bacteria obtained in the absence of metronidazole (41). Coinfection was performed as described previously (7). *F. alocis* and *P. gingivalis* inocula were prepared by mixing equal volumes (1×10^7 cells/well) of bacterial suspension which was then incubated for 5 min in the anaerobic chamber prior to infection. The serially diluted lysate was plated on BHI blood agar and incubated for 6 to 10 days. The bacterial colonies were phenotypically identified.

EM. Transmission electron microscopy (TEM) was performed using an FEI G^2 TEM per the method of Harris (42). The processed grids were placed in stain solution containing neutral 1% aqueous phosphotungstic acid for 30 s. After being blotted dry, the slides were examined using an FEI G^2 TEM.

Ultrathin sections were made per the method described by Massey (43). The trypsinized HeLa cell monolayers were pelleted and postfixed in 1% OsO_4–0.1 M sodium cacodylate for 1 h, and the ultrathin sections were contrasted using lead citrate and uranyl acetate before examination using an FEI-Technai G^2 transmission electron microscope.

Scanning electron microscopy was performed per the method described in reference 44 using a Philips XL30 FEG (FEI). The trypsinized culture of HeLa epithelial cells (5×10^3 cells/ml) was grown on coverslips in 4-well BD Falcon culture slides (BD Falcon, Bedford, MA) in Dulbecco's modified Eagle's medium (DMEM) supplemented with 10% fetal bovine serum, penicillin (100 IU/ml), streptomycin (100 IU/ml), and amphotericin B (2.5 mg/ml) (Invitrogen, Carlsbad, CA), at 37°C under 5% CO_2. The infected epithelial cells were later grown in Eagle's DMEM without serum several times to ensure complete transition from growth media to fixative, and fixation was carried for 30 min at room temperature. The processed coverslips were subjected to carbon coating using a vacuum evaporator and sputter coated. The slides were then viewed using a Philips XL30 FEG.

Sample preparation and labeling for MS. The infected epithelial cells were trypsinized followed by centrifugation at 5,000 × *g*, and the pellet was freeze-thawed twice. Approximately 300 μg of protein sample in 100 mM Tris-HCl (pH 8.6)–0.1% SDS buffer solution was reduced by incubation in 10 mM dithiothreitol (DTT) at 50°C for 1 h followed by carboxymethylation with 25 mM iodoacetamide in the dark for 2 h. Proteins were precipitated using cold acetone at −20°C overnight. The protein pellet was obtained by centrifugation at 15,000 rpm for 10 min, and the

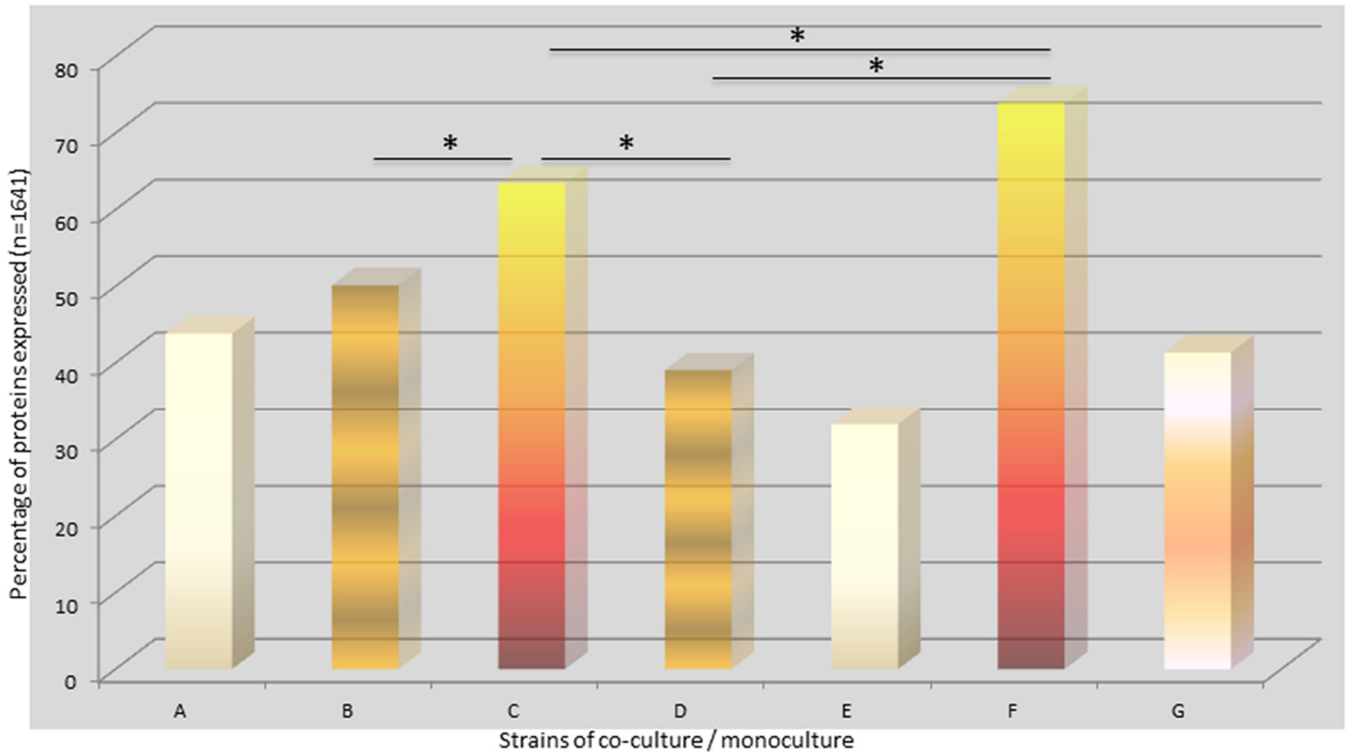

FIG 1 Percentage of protein expressed during coculture or monoculture using various strains of *P. gingivalis* and *F. alocis*. HeLa cells were infected with *F. alocis* ATCC 35896 and D-62D strains (MOI of 1:100 [10^5 epithelial cells]) in monoculture or coculture with *P. gingivalis* W83 as previously reported (6). Tandem isobaric mass tagging analysis of cocultures and monocultures was carried out using Orbitrap. (*, $P < 0.01$.) Bar A, *P. gingivalis* (33277) plus *F. alocis* (D-62D) versus *P. gingivalis* (33277) plus *F. alocis* (ATCC); bar B, *P. gingivalis* (33277) plus *F. alocis* (D-62D) versus *P. gingivalis* (W83) plus *F. alocis* (D-62D); bar C, *P. gingivalis* (33277) plus *F. alocis* (D-62D) versus *F. alocis* (D-62D); bar D, *P. gingivalis* (33277) plus *F. alocis* (ATCC) versus *P. gingivalis* (W83) plus *F. alocis* (ATCC); bar E, *P. gingivalis* (W83) plus *F. alocis* (D-62D) versus *P. gingivalis* (W83) plus *F. alocis* (ATCC); bar F, *P. gingivalis* (W83) plus *F. alocis* (D-62D) versus *F. alocis* (D-62D); bar G, *F. alocis* (D-62D).

supernatant was removed using a glass Pasteur pipette. The protein pellet was dissolved in 80 mM triethyl ammonium bicarbonate buffer. Proteins were subsequently digested using trypsin at a protein/enzyme ratio of 40:1 (by mass), and the samples were incubated at 37°C overnight. A tandem mass tag (TMT) isobaric mass tagging kit (Thermo Fisher Scientific) was used for labeling the samples following the manufacturer's recommended conditions. The U937 control protein digests were labeled with TMT labels 128 and 130, whereas the phorbol myristate acetate (PMA)-treated protein digests were labeled with TMT labels 127 and 129. Equal amounts of the labeled control and PMA-treated protein digests were combined for mass spectrometry (MS) analysis.

MS and data analysis. Protein samples were analyzed using a Thermo Scientific LTQ Orbitrap Velos mass spectrometer and the data processed as previously reported (45). The four-part protocol used for the MS and tandem MS (MS/MS) analyses was carried out, and the data collection was achieved using Xcalibur software (Thermo Electron) followed by screening performed with Bioworks 3.1.

Data processing and functional analysis. The data from the Orbitrap were processed and searched using Thermo Scientific Proteome Discoverer software suite 1.1. The MASCOT software was used for each analysis to produce unfiltered data and output files. Statistical validation of peptide and protein findings was achieved using X TANDEM (www.thegpm.org) and SCAFFOLD 2 meta-analysis software. The presence of two different peptides at a probability of at least 95% was required for consideration of a result as representing positive identification. General protein database searches were conducted using the UniProtKb protein knowledge base database (http://www.uniprot.org/uniprot). The *F. alocis* open reading frame (ORF) database is based on the latest release of the *Filifactor alocis* genome at the NCBI genome project (http://www.ncbi.nlm.nih.gov/nuccore/CP002390.1). Human protein identifications were performed using the Human IPI database (ftp://ftp.ebi.ac.uk/pub/databases/IPI) (46). A precursor ion mass tolerance of 10 ppm and fragment ion tolerance of 0.01 Da and MUDPIT scoring were applied with a peptide cutoff score of 10 and a peptide relevance score of 1. Peptides were filtered based on false-discovery-rate cutoff values of 1% (strict) and 5% (relaxed). Using MASCOT searching, 98% of the total peptides detected were quantified. Protein ratios were reported as the mean values for the observed peptides.

Functional analysis. The NCBI RefSeq symbols of the modulated genes were mapped to their corresponding gene names in Ingenuity Pathways Analysis (IPA) software (Ingenuity Systems). The corresponding lists were processed using the IPA software to arrive at the canonical pathways, biological functions, and networks significantly associated with the gene lists. Ingenuity Pathways Analysis is a knowledge database and Web-based analysis system that permits classification of the molecular networks and biological function and metabolic canonical pathways that are most significantly represented in the set of genes of interest. The *P* value associated with biological process or pathway annotation was calculated according to the right-tailed Fisher exact test. This statistical test assesses the null hypothesis that the proportion of genes that map to a particular function or pathway in the sample is similar to the proportion that map in the entire population (IPA reference set). Only overrepresented functions or pathways that are more abundant than expected by chance are reported as significant and given the respective color codes for up- and downregulation. The gene ontology classification was used for referencing the eukaryotic proteome through manual curation and also using QuickGo (www.ebi.ac.uk/quickgo/).

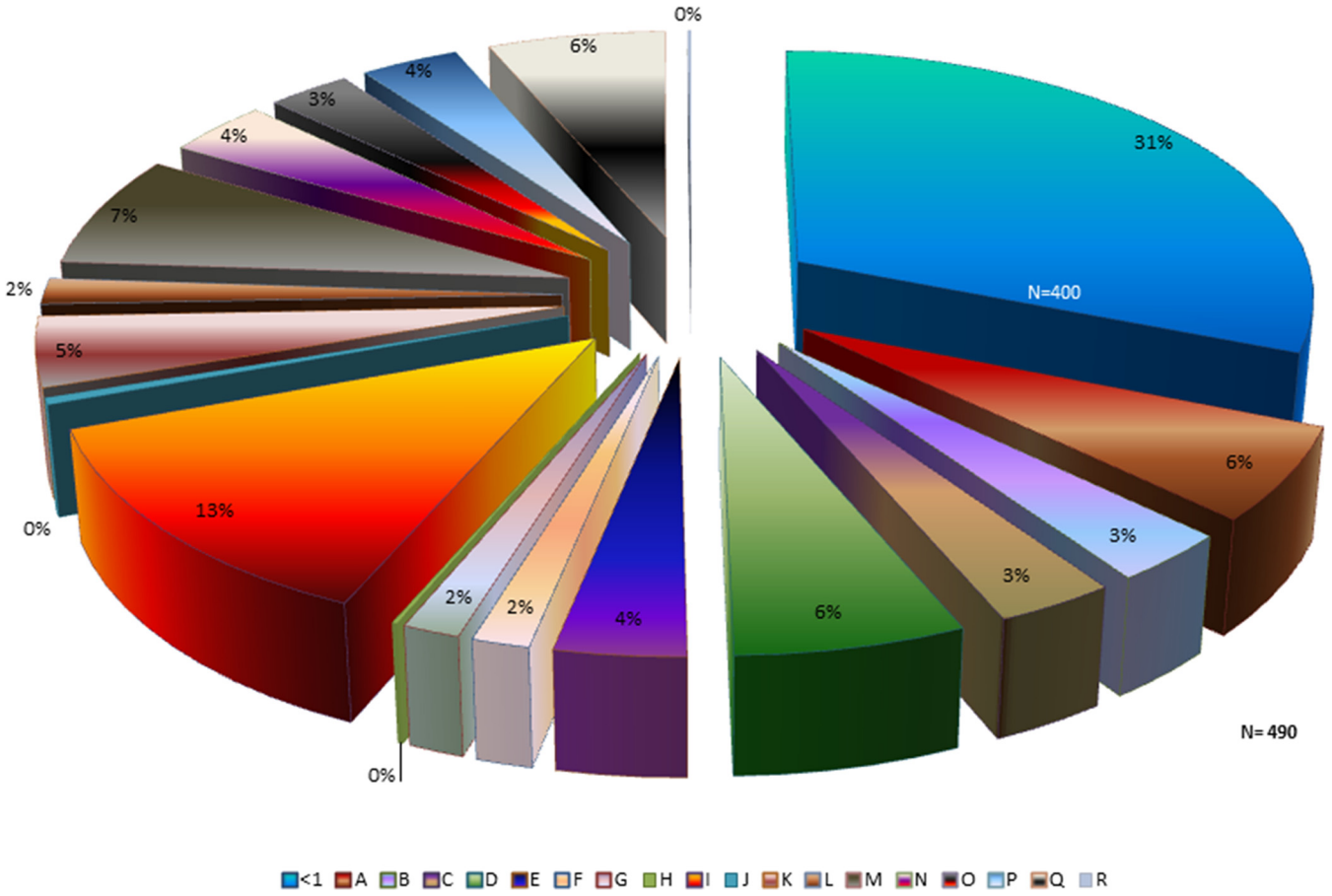

FIG 2 Upregulation in proteome profile showing various protein classes noted during coculture infection with *P. gingivalis* and *Filifactor alocis* in epithelial cells. HeLa cells were infected with *F. alocis* ATCC 35896 and D-62D strains (MOI of 1:100 [10^5 epithelial cells]) in monoculture or coculture with *P. gingivalis* W83 as previously reported (6). Tandem isobaric mass tagging analysis of cocultures and monocultures was carried out using Orbitrap. The *F. alocis* proteins were analyzed using MASCOT, and functional analysis was carried out using the UNIPROT proteome database. A, amino acid biosynthesis; B, biosynthesis of cofactors, prosthetic groups, and carriers; C, cell envelope; D, cellular processes; E, central intermediary metabolism; F, DNA metabolism; G, energy metabolism; H, fatty acid and phospholipid metabolism; I, hypothetical/unassigned/uncategorized/unknown functions; J, mobile and extrachromosomal element functions; K, protein fate; L, purines, pyrimidines, nucleosides, and nucleotides; M, regulatory functions; N, replication; O, transcription; P, translation; Q, transport and binding; R, transposon functions. Protein expression change > 1-fold, $n = 490$; protein expression change < 1-fold, $n = 400$.

RESULTS

Several proteins from *F. alocis* D-62D were increased in abundance during coinfection of epithelial cells with *P. gingivalis* W83. Because the variations in the pathogenic potential of the *F. alocis* strains in coculture with *P. gingivalis* may be related to the relative abundances of specific bacterial protein factors, we examined the proteome of *F. alocis* during coinfection of epithelial cells with *P. gingivalis*. As shown in Fig. 1, approximately 20% to 30% (comparing bars C and F with bar G) more proteins were observed in *F. alocis* during coinfection with *P. gingivalis* ($P < 0.01$). Unlike *F. alocis* ATCC 35896, the D-62D strain expressed more proteins interacting with *P. gingivalis* W83 than with *P. gingivalis* 33277. The proteome modulation of *F. alocis* during coinfection with *P. gingivalis* W83 showed a total of 490 proteins with a change in expression of >1-fold in contrast to 400 proteins that had a change in expression of 0.5-fold to 1.0-fold. The proteins that were most highly upregulated were classified as hypothetical (13%), regulatory (7%), and transport and binding (6%) proteins and related to cellular processes (6%) and amino acid biosynthesis (6%) (Fig. 2). Several surface adhesion proteins that were upregu-

TABLE 1 *F. alocis* coinfection with *P. gingivalis*: relative abundance of proteins with cell wall motif

Annotation	Name
HMPREF0389_01580	Leukotoxin translocation ATP binding protein
HMPREF0389_00575	Fibronectin binding protein
HMPREF0389_00426	Type IV pilus assembly protein
HMPREF0389_00816	Signal recognition particle protein
HMPREF0389_01719	Hypothetical protein
HMPREF0389_00599	Hypothetical protein
HMPREF0389_00019	Hypothetical protein
HMPREF0389_01532	Calcium binding acid repeat protein
HMPREF0389_01139	S-layer Y domain-containing protein
HMPREF0389_00672	Hypothetical protein
HMPREF0389_01172	Hypothetical protein
HMPREF0389_00415	Fimbrial assembly protein
HMPREF0389_01657	Membrane protein
HMPREF0389_01476	Hypothetical protein
HMPREF0389_01477	Hemolysin III type calcium binding protein
HMPREF0389_01478	Protein export membrane protein
HMPREF0389_01006	Collagen adhesion protein

TABLE 2 *F. alocis* proteins found in relative abundance during coinfection

Gene ID	Annotation	Fold change	
		D-62D	ATCC
HMPREF0389_00905	Sodium neurotransmitter symporter family protein	3.64	2.76
HMPREF0389_00296	PP loop family protein	6.38	1.15
HMPREF0389_01047	TetR family transcriptional regulator	1.75	1.04
HMPREF0389_01180	Anti-anti-sigma factor RsbV	2.92	1.09
HMPREF0389_00038	Hypoxanthine phosphoribosyl transferase	1.70	2.09
HMPREF0389_01084	Hypothetical protein (containing −7TM receptors with diverse intracellular signaling molecules)	1.63	1.20
HMPREF0389_01060	GMP synthase	1.63	1.10
HMPREF0389_01081	Caax aminoprotease family protein	1.68	1.75
HMPREF0389_00290	Translational regulator LacI family	2.38	1.20
HMPREF0389_01109	FeS assembly ATPase SufC	2.08	1.50
HMPREF0389_01107	Iron-regulated ABC-type transporter	1.51	2.5
HMPREF0389_00519	Hypothetical protein (containing putative zinc ribbon domain)	2.18	3.3
HMPREF0389_00052	CDP-diacyl glycerol-glycerol 3 phosphate 3 phosphatidyl transferase	2.06	1.90
HMPREF0389_00948	Phosphoglycerate dehydrogenase	1.95	1.52
HMPREF0389_01590	Transcriptional regulator AraC family	1.55	1.03
HMPREF0389_01398	Oxygen-independent coproporphyrinogen III oxidase	1.83	1.08
HMPREF0389_01164	Hypothetical protein	2.28	1.31
HMPREF0389_00472	Gamma glutamyl ligase family	1.92	1.40
HMPREF0389_00387	Pyruvate kinase	2.47	0.74
HMPREF0389_00382	Hypothetical protein (VCBS domain protein)	4.11	1.13
HMPREF0389_00294	Ribose ABC transporter permease protein	1.74	2.4
HMPREF0389_00212	CRISPR-associated protein 2 Cas2	2.12	1.4
HMPREF0389_00211	CRISPR-associated protein 1 Cas1	1.4	0.70
HMPREF0389_00210	CRISPR-associated protein Csn1	1.046	1.00
HMPREF0389_01169	CRISPR-associated protein Csd1	0.960	0.95
HMPREF0389_01170	CRISPR-associated protein Cas5	0.748	0.78
HMPREF0389_01165	CRISPR-associated protein Cas2	1.30	1.20
HMPREF0389_01167	CRISPR-associated protein Cas4	1.01	1.00
HMPREF0389_00275	Peptidyl prolyl isomerase	1.243	1.0
HMPREF0389_01236	30S ribosomal protein S18	3.9	1.5
HMPREF0389_00068	Hypothetical protein	1.8	1.1
HMPREF0389_00044	Glutamate synthase, RluA family	2.08	0.8
HMPREF0389_00019	Outer membrane protein	2.34	1.8
HMPREF0389_00569	tRNA delta(2) isopentenyl pyrophosphate/glucosamine 1 phosphate N acetyltransferase	1.83	1.1
HMPREF0389_00756	Cytidylate kinase	1.70	2.3
HMPREF0389_00967	Hypothetical protein (CHASE 3 domain)	3.10	6.4
HMPREF0389_00243	Toxin-antitoxin component ribbon-helix-helix fold protein	0.821	0.88
HMPREF0389_00201	Hypothetical protein (HTH3 domain protein)	1.38	1.36
HMPREF0389_00275	Peptidyl prolyl isomerase	1.24	0.99
HMPREF0389_00359	Peptidyl prolyl *cis-trans* isomerase	1.24	1.10

lated during coinfection include collagen adhesion protein, fibronectin binding protein, calcium binding acid repeat proteins, and hemolysin III calcium binding protein. Furthermore, many hypothetical proteins with cell wall anchor motifs (HMPREF0389_1719, HMPREF0389_00599, HMPREF0389_00019, HMPREF0389_00672, HMPREF0389_1172, and HMPREF0389_1476) were also found in abundance. The hypothetical protein HMPREF0389_00967 was highly (6.4 times) upregulated in coinfection of *F. alocis* clinical strain D-62D with *P. gingivalis* W83 (Table 1).

Upregulation of *F. alocis* proteins involved in host cell signaling. *F. alocis* strains ATCC-35896 and D-62D cocultured with *P. gingivalis* showed upregulation of bacterial proteins that are reported to be involved in eukaryotic transcription (Table 2). Coinfection also showed relative abundances of noncoding RNAs such as clustered regularly interspaced short palindromic repeat (CRISPR) RNA and toxin-antitoxin system proteins. Peptidyl prolyl *cis-trans* isomerase, an enzyme involved in the histone-modifying pathway, was also upregulated. Relevant gene network data based on host proteome data mining suggest upregulation of host cell signal transduction processes; however, analysis also showed downregulation of kinase and protein binding activities. Many vital cellular processes such as phosphorylation, apoptosis, gene expression, cell proliferation, and cell growth were modulated (see Fig. S1 and S2 in the supplemental material).

Proteome profile of epithelial cells coinfected with *F. alocis* and *P. gingivalis*. Epithelial cells coinfected with *F. alocis* and *P. gingivalis* strains showed activation of several eukaryotic proteins involved in the inflammatory response, cell signaling, and cell death (Fig. 3). The global proteome analysis of the host showed modulation in expression of 209 proteins. Among them, proteins involved in cytoskeleton organization and biogenesis were affected most (17%) followed by proteins involved in the regulation of gene expression and epigenetic modification (9%), regulation

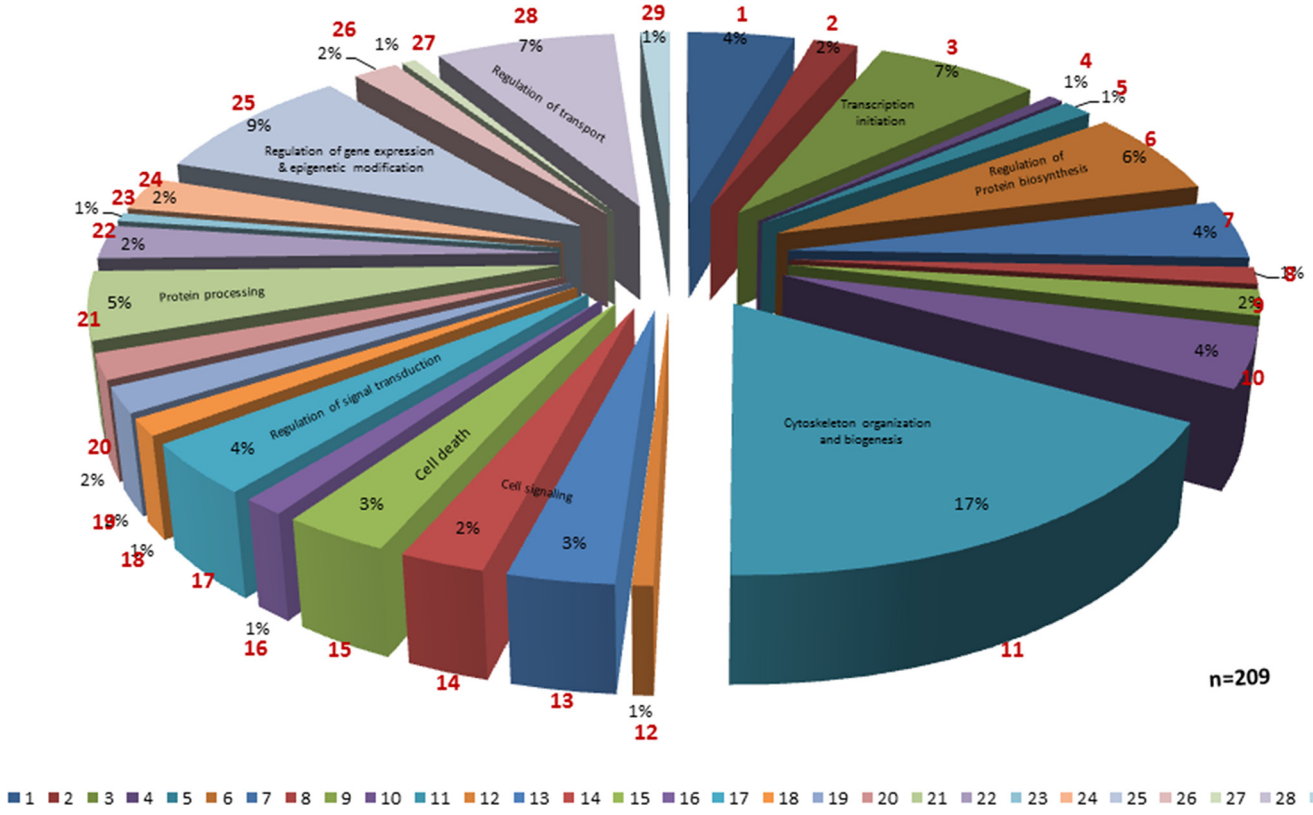

FIG 3 Eukaryotic proteome profile showing various protein classes modulated during coculture infection with *P. gingivalis* and *Filifactor alocis*. Section 1, GO:0005975 (carbohydrate metabolism); section 2, GO:0006260 (DNA replication); section 3, GO:0006352 (transcription initiation); section 4, GO:0006353 (transcription termination); section 5, GO:0006360 (transcription from RNA polymerase I promoter); section 6, GO:0006417 (regulation of protein biosynthesis); section 7, GO:0006457 (protein folding); section 8, GO:0006512 (ubiquitin cycle); section 9, GO:0006839 (mitochondrial transport); section 10, GO:0007005 (mitochondrion organization and biogenesis); section 11, GO:0007010 (cytoskeleton organization and biogenesis); section 12, GO:0007047 (cell wall organization and biogenesis); section 13, GO:0007166 (cell surface receptor-linked signal transduction); section 14, GO:0007264 (small-GTPase-mediated signal transduction); section 15, GO:0008219 (cell death); section 16, GO:0009890 (negative regulation of biosynthesis); section 17, GO:0009966 (regulation of signal transduction); section 18, GO:0015931 (vesicle organization and biogenesis);section 19, GO:0016071 (mRNA metabolism); section 20, GO:0016481 (negative regulation of transcription); section 21, GO:0016485 (protein processing); section 22, GO:0018193 (peptidyl amino acid modification); section 23, GO:0019932 (secondary messenger-mediated signaling); section 24, GO:0030705 (cytoskeleton-dependent intracellular transport); section 25, GO:0040029 (regulation of gene expression, epigenetics); section 26, GO:0045333 (cellular respiration); section 27, GO:0045454 (cell redox homeostasis); section 28, GO:0051049 (regulation of transport); section 29, GO:0051052 (regulation of DNA metabolism).

of protein transport (7%), transcription initiation (7%), regulation of protein biosynthesis (6%), protein processing (5%), regulation of signal transduction (4%), and cell death-apoptosis (3%). Highly downregulated proteins during coinfection include eukaryotic translation initiation factor, splicing factors, histone protein clusters, and other signaling proteins such as vimentin, prohibitin, and redox proteins. Highly upregulated proteins include the RAS oncogene family proteins, proteins involved in granzyme signaling, and cytoskeletal matrix proteins (Table 3). An Ingenuity pathway analysis showed increased expression of eukaryotic genes involved in antigen presentation, cellular movement, the hematological system, cell trafficking, and inflammatory response (see Fig. S3 in the supplemental material).

Many host cell regulatory proteins that are involved in cytoskeleton integrity were modulated. The integrin beta-1 (ITGB1) genes are downregulated in coculture. The valosin-containing protein (VCP) gene involved in ubiquitin-dependent protein degradation is downregulated in coculture. In both coculture and monoculture of *F. alocis*, there was upregulation of the poly-β-hydroxybutyrate (PHB) gene involved in negative regulation of cell proliferation (see Fig. S4 in the supplemental material). The vinculin (VCL) gene coding for the membrane cytoskeleton protein vinculin and the voltage-dependent anion channel (VDAC1) gene were upregulated during coinfection. Proteins involved in important cell regulatory networks such as serine/arginine-rich splicing factor 1 (SRSF1), annexin-2 (ANXA2), heat shock proteins (HSPA8, HSP9, and HSPE1), synaptotagmin binding protein (SYNCRIP), eukaryotic initiation factor 4A-1, 19-kDa protein-SRP-dependent translational protein, protein S100A11, and other cytoskeletal proteins such as the lamin A/C proteins were also found to be modulated (see Table S2). There was a generalized downregulation of the actin pathway (see Fig. S5).

In order to identify variations in host cell surface morphology and cell death between coinfection and monoinfection, epithelial cells coinfected with *F. alocis* and *P. gingivalis* were subjected to electron microscopy study. Wide morphological variation of the host cell was noted after coinfection compared to monoinfection with either *F. alocis* or *P. gingivalis*. The infected epithelial cells show modification of cell surface filopodial projections that were used by both *F. alocis* and *P. gingivalis* to adhere to the cell surface

TABLE 3 Modulated host proteins during coinfection with *F. alocis* and *P. gingivalis*

Gene	Fold change	Annotation
Downregulated proteins		
EIF4B	−3.675	Eukaryotic translation initiation factor 4B
HIST1H1C	−2.742	Histone cluster 1, H1c
HIST1H1E	−2.643	Histone cluster 1, H1e
HIST1H2BL	−2.790	Histone cluster 1, H2bl
PPIA	−3.307	Peptidyl prolyl isomerase A (cyclophilin A)
VIM	−2.158	Vimentin
SRSF1	4.049	Serine/arginine-rich splicing factor 1
PHB		Prohibin
TRAP 1	−1.035	TNF receptor-associated protein 1
PRDX1	−1.219	Peroxiredoxin 1 and 5
PRDX5	−1.201	
Upregulated proteins		
NACA	2.310	Nascent polypeptide-associated complex alpha subunit
IMPDH2	2.472	Inosine-5′-monophosphate dehydrogenase 2
AGF3	1.774	AFG3-like protein 2
RAB 10	1.128	Member of RAS oncogene family
RAB 7A	1.028	Member of RAS oncogene family
ITGB1	1.356	Integrin
PHB	1.260	Prohibitin
VCL	2.189	Vinculin
IGAAD		Granzyme A signaling proteins
HSP10	2.160	10-kDa heat shock protein (mitochondrial)
LDHA	1.516	Isoform 1 of L-lactate dehydrogenase A chain
	1.512	46-kDa protein
	1.907	26-kDa protein
NACA	2.310	Nascent polypeptide-associated complex
KRT1	1.461	Keratin type II cytoskeletal I
HNRPR	1.728	Heterogenous nuclear ribonucleoprotein R

and formation of membrane microdomains such as the lipid rafts (Fig. 4, panels 1 and 2). Infected cells showed early apoptosis during coinfection compared to monoinfection (Fig. 4A to L). Surface modifications of the coinfected epithelial cells were noted in both *F. alocis* ATCC 35896 and the clinical strain D-62D; however, the level of filopodial projections was greater in the *F. alocis* D-62D strain than in the *F. alocis* ATCC 35896 strain (Fig. 4O and P). Such morphological variations were not noted in monoinfected epithelial cells (Fig. 4M and N).

Many host proteins involved in chromatin function and remodeling were downregulated during *F. alocis* coinfection with *P. gingivalis*. An overall downregulation of histone cluster proteins and PPIA-peptidyl prolyl isomerase was noted (Fig. 5) (Table 2). The relative expression levels of such proteins were the lowest in *F. alocis* clinical strain coinfection compared to the type strain coinfection (data not shown). Heterogeneous nuclear ribonuclear protein A2/B1 was found in least abundance during coinfection. Proteins involved in transport and secretory pathways such as the transferrin receptor protein 1 (involved in iron transport), transmembrane emp24 domain-containing protein 10 and dynein (involved in vesicular protein trafficking), surfeit 4, and solute carrier family proteins were also less expressed during coinfection.

Proteins that are known to activate oncogenes directly or indirectly were expressed in high abundance during *F. alocis* coculture. The major proteins that were present in high abundance during coinfection were RAB 7A, RAB10 proteins belonging to the RAS oncogene family, poly(rC) binding protein 2 (PCBP2), voltage-dependent anion channel protein 1, copine-1 (calcium-dependent membrane binding protein), and collagen alpha-2 (V) chain precursor (Table 3).

Many host cell proteins that are involved in cell adhesion and cytoskeletal interactions were upregulated during coinfection of *F. alocis* with *P. gingivalis*. Host cytoskeletal proteins such as vimentin, actin, plectin, vinculin, profilin, and transgelin and chaperone proteins such as HSP90 and endoplasmin and proteins such as filamin B and filamin C involved in cell communication were modulated. Signal transduction proteins galectin, proteasome subunit alpha type 6, and 14-3-3 protein theta were relatively less abundant. Inosine 5′ monophosphate dehydrogenase (IMPDH), receptor kinectin, and peroxiredoxins were found to be highly expressed during coinfection (see Table S2).

Oribtrap analysis of the whole proteome of *F. alocis* coculture with *P. gingivalis* revealed many upregulated host cell proteins that are involved in apoptosis, cell regulation, and differentiation pathways. Proteins such as prohibitins and Ras-related protein Rab 10 and Ras-related protein Rab 7 SET translocation proteins that are involved in apoptosis and histone binding were upregulated. Also, SRSF1 protein encoded by a proto-oncogene, nascent-polypeptide-associated complex alpha (NACA) protein (transcriptional coactivator), NPM1 (nucleophosmin) involved in apoptosis and tumorigenesis, and CALR (calreticulin) involved in calcium binding and storage were highly upregulated (Fig. 6). Further, our analysis showed upregulation of proteins involved in the ubiquitin proteasome pathway and the granzyme-mediated apoptotic signaling pathway (see Fig. S6 in the supplemental material).

The host metabolic pathways modulated during coinfection are given in Table 4. Pathways relating to ammonia synthesis, urate biosynthesis, amino acid degradation (valine and aspartate), lipid synthesis, and palmitate and fatty acid synthesis were highly upregulated. There was downregulation of amino acid excretory pathways and transport pathways such as the glutamyl/arginine exchange and tryptophan pathway. Coinfection of *F. alocis* was shown to affect basic energy pathways such as glycolysis and acetyl coenzyme A (CoA) biosynthesis.

DISCUSSION

F. alocis and *P. gingivalis* are important members of a complex multispecies biofilm that occupies the gingival crevice. Multiple interbacterial interactions are required for developing and maintaining the subgingival microbial community (47, 48). The impact of these interspecies interactions on the host is significant for their survival and their ability to cause disease. In contrast to previous approaches that have used purified proteins and isogenic mutants to identify specific molecular pathways responsible for many of the complex cellular responses involving host-microbe interactions, this study has used a comprehensive proteomic assessment that simultaneously evaluated the modulation of proteins in key pathways in both the microbe and the host. We previously reported variations in the pathogenic potential of *F. alocis* strains which may be partly related to the differential expression of several putative virulence factors, including several proteases, neutrophil activating protein A, and calcium binding acid repeat pro-

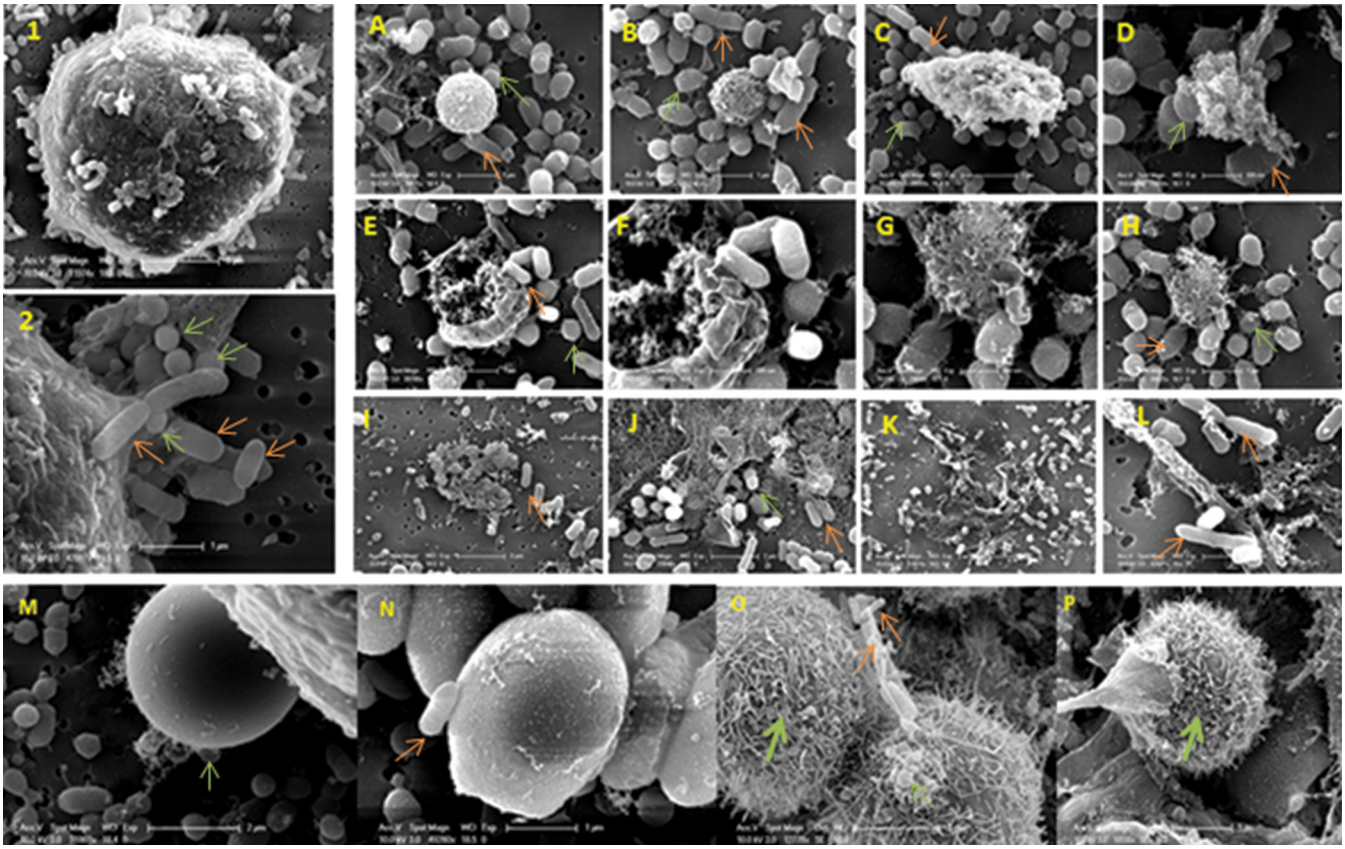

FIG 4 Coinfection of *P. gingivalis* and *Filifactor alocis*, showing morphological variations during adherence leading to apoptosis of the epithelial cells. Scanning electron microscopy images show modification of the cell surface with filapodial projections in infected epithelial cells that were used by both *F. alocis* and *P. gingivalis* to adhere to the cell surface (panels 1 and 2). Infected cells showed early apoptosis during coinfection compared to monoinfection (A to L). Surface morphological variations were not noted in monoinfected epithelial cells (M and N). Filopodial projections were more increased in the *F. alocis* D-62D strain (O and P). Orange arrows, *F. alocis*; light-green arrows, *P. gingivalis*; dark-green arrows, filapodial projections.

tein (36). Expression of these factors was increased during the invasion of HeLa cells (23).

In this study, *F. alocis* in coculture with *P. gingivalis* showed enhanced adhesion to epithelial cells, altering the cell morphology and inducing cell death. This was in contrast to monoinfections with either *F. alocis* or *P. gingivalis*, which did not trigger the same morphological alteration, although the monoinfections were still able to induce cell death over a longer time period. These observations are consistent with previous reports which showed that the virulence potential of *F. alocis* is enhanced by its coinfection with *P. gingivalis* (23, 36). While there was uniform expression of several membrane proteins that might play a role in attachment and virulence modulation (23), proteomic analysis of *F. alocis* during coinfection of epithelial cells with *P. gingivalis* revealed upregulation of several membrane adhesion proteins. This suggests that the interaction of *F. alocis* and *P. gingivalis* may result in the upregulation of a specific factor(s) that may enhance its virulence potential. Furthermore, several of these proteins are structurally related to other microbial surface component-recognizing adhesion matrix molecules (MSCRAMMs) that are known to play an important role in Gram-positive bacterial virulence by mediating adherence to and colonization of host tissues, which are early steps in clinical infection (49). Given the relative abundances of the many collagen binding MSCRAMMs, this may suggest that collagen is a likely target for *F. alocis*. Several unique hypothetical proteins with transmembrane domains were also observed to be upregulated. Proteins with these domains show interaction with extracellular matrix components which in turn can act as proinflammatory signal molecules (50). It is also noteworthy that there are no homologues of these proteins identified in *P. gingivalis*. Their functional role in *F. alocis* pathogenesis is under further investigation in the laboratory.

There is evidence that extracellular matrix adhesion proteins can be regulated by quorum sensing (51), which implies that environmental signals can modulate their expression and hence adhesion and colonization. Putative *F. alocis* proteins that could be involved in quorum sensing and signal transduction pathways were upregulated during coinfection. One of the highly upregulated hypothetical proteins, HMPREF0389_00967, contains a CHASE3 extracellular sensory domain. This domain, which is commonly found in histidine kinase, adenylate cyclases, and chemotaxis proteins (52), is involved in signal transduction pathways in bacteria (53). It is tempting to speculate that this protein plays a role in cell signaling and mediation of quorum sensing. Some of the other major proteins upregulated during coinfection include the noncoding RNA, CRISPR RNA, and toxin-antitoxin system proteins. CRISPR regulation of gene expression (54) is implicated in biofilm formation (55) and horizontal gene transfer (56, 57) in

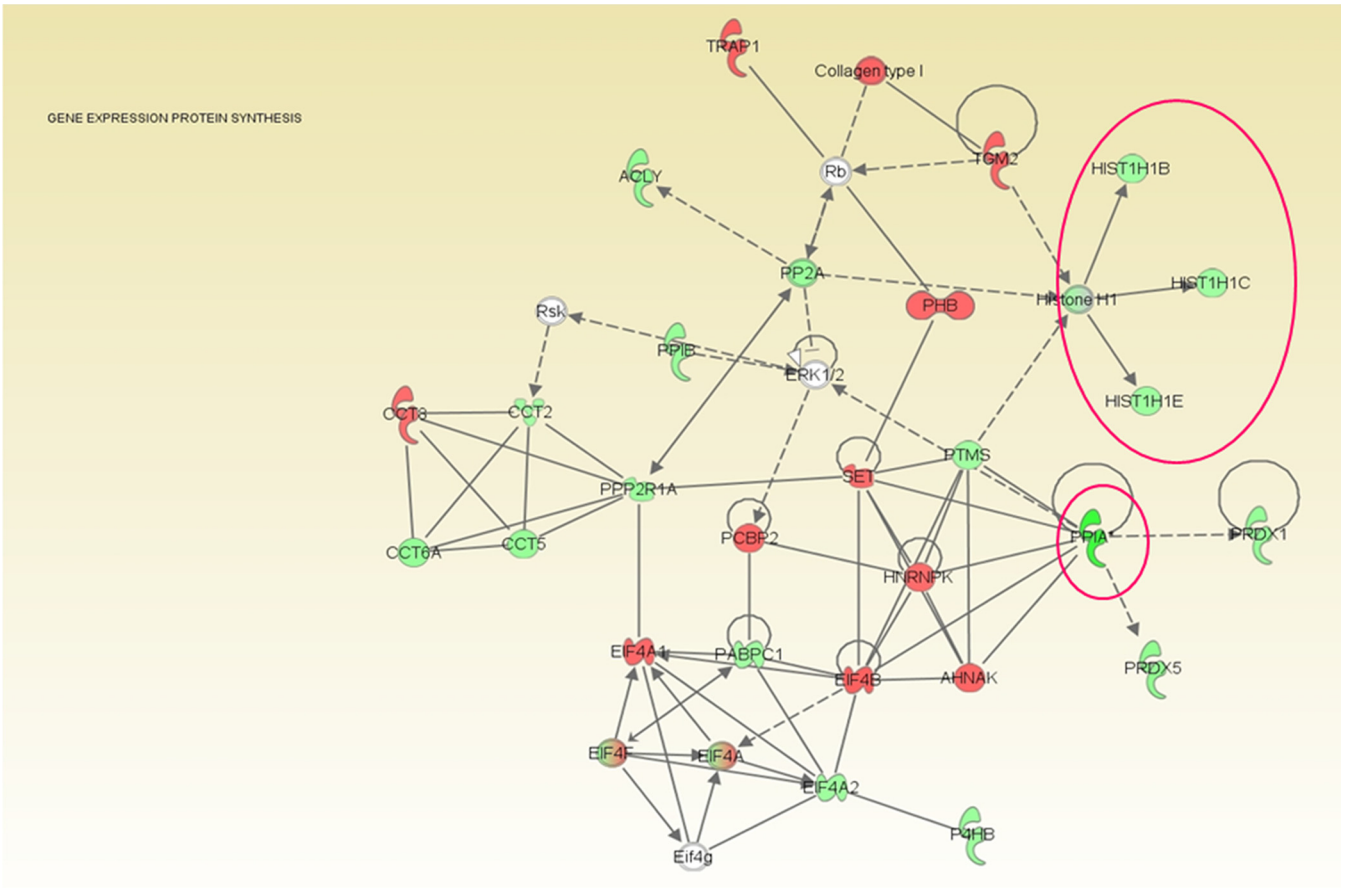

FIG 5 Coinfection of *Filifactor alocis* with *P. gingivalis* showing downregulation of proteins involved in gene expression and protein synthesis pathways. HeLa cells were infected with the *F. alocis* ATCC 35896 and D-62D strains (MOI of 1:100 [10^5 epithelial cells]) in monoculture or coculture with *P. gingivalis* strains as previously reported (6). Tandem isobaric mass tagging analysis of cocultures and monocultures was carried out using Orbitrap. The eukaryotic proteins were analyzed using MASCOT, and functional analysis was carried out using Ingenuity pathway analysis software. The gene ontology classification was used for referencing the proteome. *F. alocis* coinfection with *P. gingivalis* showed overall downregulation of histone cluster proteins (histone [Hist] H1, Hist 1H1B, Hist 1H1C, and Hist 1H1E) (shown within the circle), peptidyl prolyl isomerase (PPIA and PPIB), and antioxidant enzymes (PRDX1 and PRDX5). Green, downregulation; red, upregulation; solid lines, direct interaction; dotted lines, indirect interaction.

other oral bacteria. These proteins have also been implicated in stress response and chaperone function, mediating important signal transduction events (58). It was also noted that HMPREF0389_00382, a hypothetical protein that contains two VCBS domains (repeat domains in *Vibrio*, *Colwellia*, *Bradyrhizobium*, and *Shewanella*), was highly upregulated. These VCBS domain-containing proteins are involved in bacterial adhesion and play a role in virulence in other pathogenic bacteria (TIGRfam1965).

Our coinfection study showed relative abundances of many bacterial methyltransferases which could imply that they may play a role in targeting host DNA hypermethylation and chromatin modification. Similar variations in protein expression were also noted in a previous study performed with gingival epithelial cells coinfected with *P. gingivalis* and *F. nucleatum* (59). Note that histone modification through the mitogen-activated protein kinase (MAPK) pathway was found to be mediated by peptidyl prolyl *cis-trans* isomerase in other pathogenic bacteria (60). Both *P. gingivalis* and *F. alcois* possess the gene coding for peptidyl prolyl *cis-trans* isomerase (36). Our study showed increases in the abundance of these proteins during coinfection. Further, our study also showed variations in the host proteins that are involved indirectly in chromatin modification during *F. alocis* coinfection with *P. gingivalis*. Coinfection showed relative abundances of proteins such as parathymosin, prothymosin a14, prothymosine alpha (PTMA), SET translocation protein, and zinc finger BED domain-containing protein 1 that affect histone binding to nucleosomes causing histone binding (61) and chromatin remodeling (62). These proteins also regulate histone acetylation (63). Bacterially induced DNA methylation was shown earlier to affect the host cell proliferation (64). While host-pathogen methyltransferase similarities among many virulent strains of bacteria were noticed earlier (65), chromatin modification through bacterial proteins can regulate expression of host genes and enzymes such as histone deacetylase (HDAC) (66). Such DNA methylation and histone acetylation are commonly associated with cancer and tumor growth (59). The *F. alocis* genome is annotated with 18 methyltransferase genes; their role in host chromatin modification and epigenetic changes awaits further confirmation. Our study showed upregulation of many methyltransferase genes during coinfection.

Coinfection of *F. alocis* with *P. gingivalis* showed modulation of

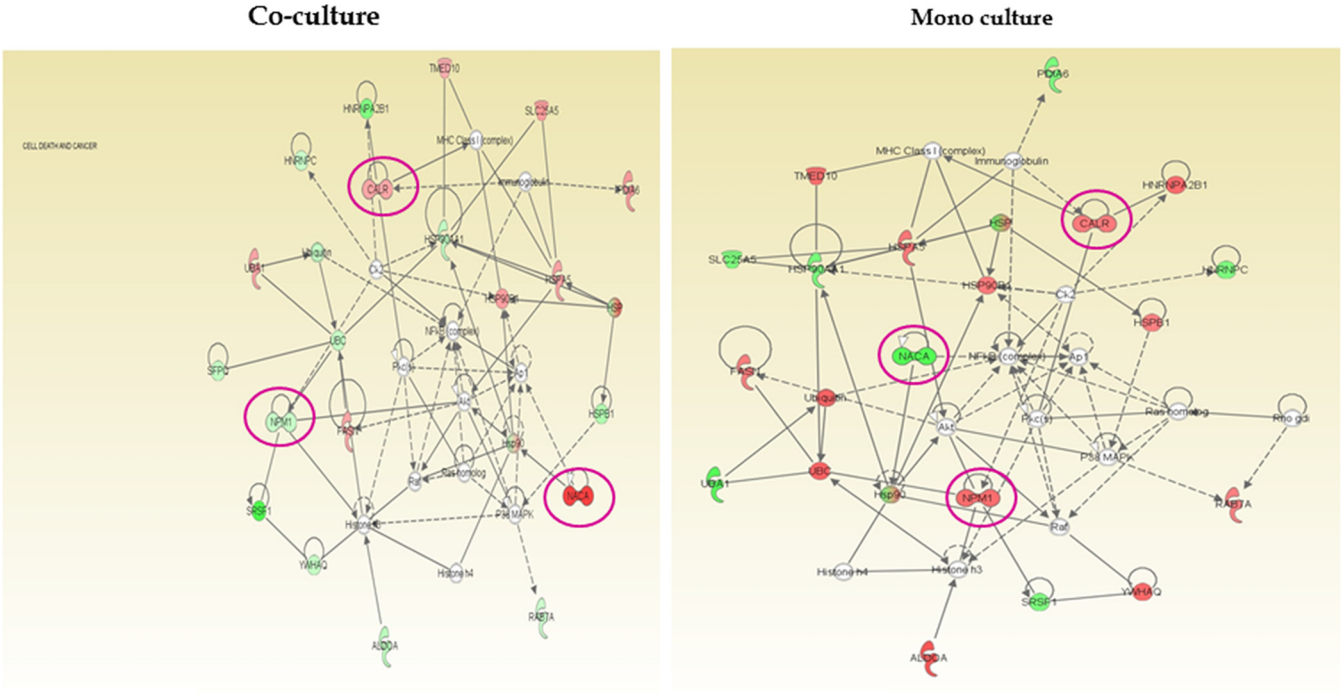

FIG 6 Coinfection of *Filifactor alocis* with *P. gingivalis* showing upregulation of proteins involved in cancer and cell death pathways. HeLa cells were infected with *F. alocis* ATCC 35896 and D-62D strains (MOI of 1:100 [10^5 epithelial cells]) in monoculture or coculture with *P. gingivalis* strains as previously reported (6). Tandem isobaric mass tagging analysis of cocultures and monocultures was carried out using Orbitrap. The eukaryotic proteins were analyzed using MASCOT, and functional analysis was carried out using Ingenuity pathway analysis software. The gene ontology classification was used for referencing the proteome. Proteins such as prohibitins, Ras-related protein Rab 10, and the Ras-related protein Rab 7 SET translocation protein that are involved in apoptosis and histone binding were upregulated. Also, the SRSF1 protein encoded by a proto-oncogene, NACA protein (transcriptional coactivator), NPM1 (nucleophosmin; involved in apoptosis and tumorigenesis), and CALR (calreticulin; involved in calcium binding and storage) were highly upregulated. Green, downregulation; red, upregulation.

TABLE 4 Metabolome variation in host protein during *F. alocis* coinfection

Expression category and pathway
Upregulated
Ammonia production
Urate biosynthesis through inosine 5′phosphate degradation
Valine degradation
Aspartate degradation
L-Asparagine synthesis
Glutaraldehyde CoA degradation
Fatty acid biosynthesis
Pentose phosphate pathway
TCA cycle[a]
Pyruvate fermentation to lactate
Thioredoxin pathway
Palmitate biosynthesis
Purine *de novo* synthesis
Downregulated
Sodium-independent glutamyl/arginine exchange
L-Tryptophan transport
Sucrose degradation
Peptidyl proline synthesis
Phosphoprotein synthesis
Acetyl CoA biosynthesis from citrate
Glycolysis
NADH repair

[a]TCA, tricarboxylic acid.

host proteins involved in signaling, cell-cell interaction, and chaperone function. Several proteins involved in maintaining cell shape and the integrity of the cytoplasm and in stabilizing cytoskeletal interactions and cellular integrity were downregulated. This is correlated with the results of the electron microscopic study, which revealed variations in cell surface morphology in epithelial cells coinfected with *F. alocis* and *P. gingivalis*. Formations of lipid rafts due to the host cell plasma membrane response to pathogens were demonstrated in several invasive pathogens (67–70). Such modifications of the host cell could be used as a protective mechanism for both *F. alocis* and *P. gingivalis* to evade the degradative lysosomal pathway (69). The electron microscopy findings could be corroborated with the proteome data showing modulation of actin and other proteins involved in cytoskeletal modification. Such characteristic cytoskeletal remodeling and transcellular processes mediated by *F. alocis* could help in cointernalization of *F. alocis* and *P. gingivalis*. The increase in adhesion of *F. alocis* observed in this study would likely be due to expression of host adhesion proteins such as vinculin and VDAC1 protein that could favor pathogen adherence (71). Compared to monoinfection, coinfection with *P. gingivalis* showed an overall dysfunction of protein function and transport due to a generalized downregulation of many host chaperone proteins such as Hsp90 (heat shock protein 90), protein disulfide isomerase, and endoplasmins. Note that proteins involved in cell growth and proliferation were also affected during coinfection.

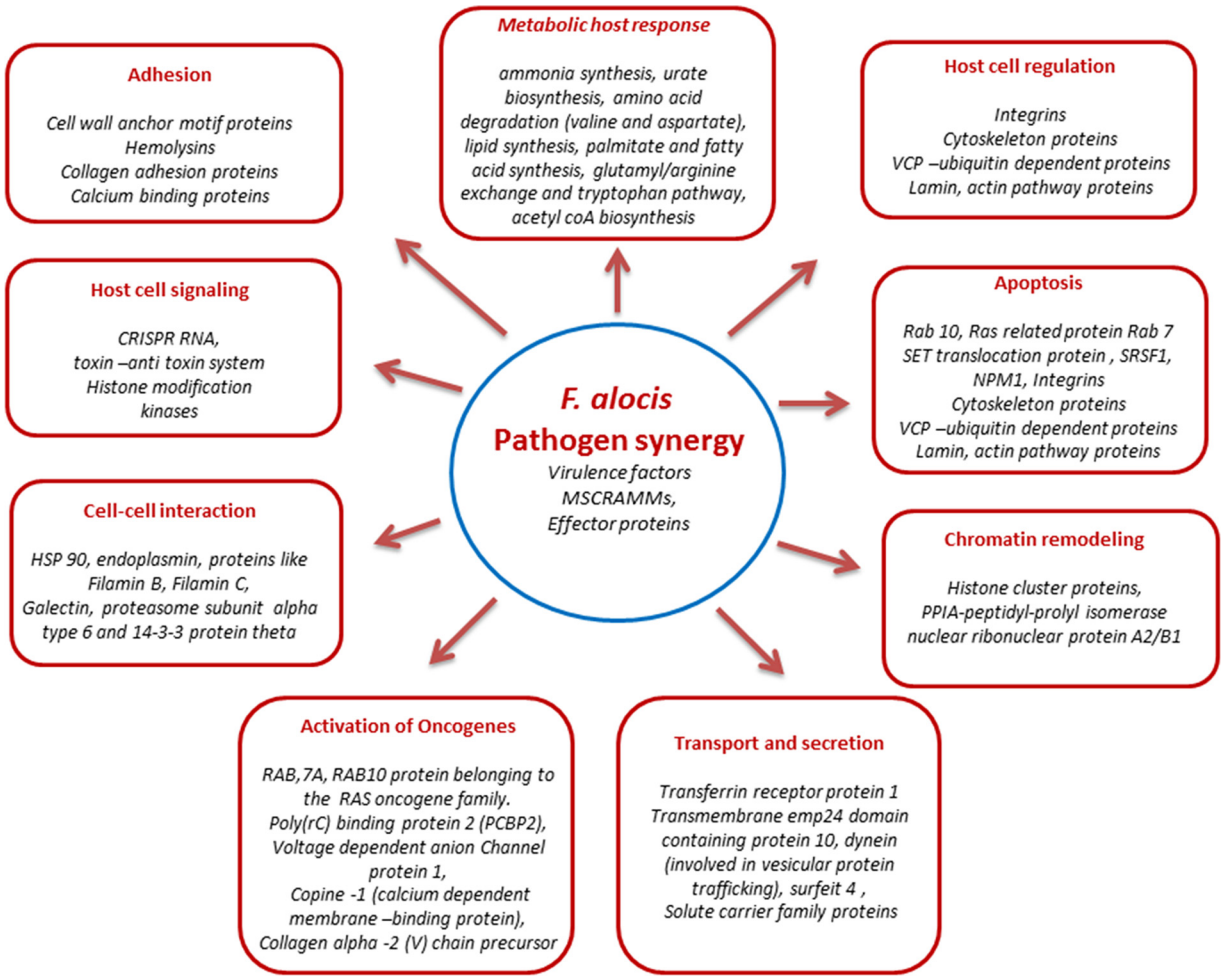

FIG 7 Summary overview showing the major role of *F. alocis* pathogen synergy in the host cell response. The major modulated proteins are shown under each category heading.

Coinfection of *F. alocis* with *P. gingivalis* showed regulation of many proteins that are involved in the host regulatory network. Among them, serine/arginine-rich splicing factor 1 (SRSF1) protein was highly downregulated. This protein imparts genomic stability and prevents slicing variants and is also implicated in many critical functions such as cell viability and programmed cell death (72). Annexin was found to be downregulated in coculture compared to monoculture. Annexin is believed to be involved in membrane-related functions of the cell and in the endocytic pathway, regulating the onset of cell degradation (73). Other major variations during coinfection include downregulation of lectin galactose binding soluble protein 1 (LGALS1), annexin 2 (ANXA2), heat shock proteins (HSPA8, HSP9, and HSPE1), and synaptotagmin binding protein (SYNCRIP). Eukaryotic initiation factor 4A-1 is involved in the cytokine-mediated signaling pathway and in host-pathogen interaction. The relative abundances of lamin A/C proteins were much lower during coinfection. They are essential proteins that make up the nuclear matrix and are involved in nuclear stability, chromatin structure, and gene expression and in lamin-associated signaling pathways. Additionally, we have noted downregulation of host cell nuclear ribonuclear proteins. These nuclear envelope (NE) proteins act as regulators of MAPK, Wnt–β-catenin, transforming growth factor β (TGF-β), and Notch signaling cascades (74). It is noteworthy that protein S100A11, implicated as a potential biomarker of infective endocarditis, was more abundant during *F. alocis* monoinfection (75). S100A11 proteins are involved in endocytosis and exocytosis (76), regulation of enzyme activity, cell growth regulation, apoptosis, and inflammation (77). Periodontitis is an inflammatory disease; however, its role in other systemic inflammatory diseases is unknown.

Metabolic host responses to bacterial infections favor survival and are important in the pathogenic process (78). The relative abundances of proteins involved in arginine metabolism and citrulline synthesis, namely, arginine deiminase (HMPREF0389_01584), acetyl ornithine transferase (HMPREF0389_01570) (36), aminotransferase (HMPREF0389_01352 and HMPREF0389_01353), amidotransferase family protein (HMPREF 0389_00349), arginine-tRNA ligase (HMPREF0389_00390), and arginine decarboxylase (HMPREF0389_00102), indicate that the nutritional needs of the bacteria are met during infection. Since *F. alocis* and *P. gingivalis* are asaccharolytic in nature and resort to protein breakdown for energy and survival, this process could lead to a heavy production of ammonia. A well-developed arginine cycle

noted in *F. alocis* could help the coinfected pathogen partners to survive well in periodontal pockets by utilizing the toxic metabolites of the host cell. This could be one of the many processes that lead to pathogen synergy. *F. alocis* genome annotation also showed *F. alocis* to possess a well-developed citrulline synthesis mechanism from arginine. Citrullination of proteins has already been shown to be an important posttranslational modification. Upregulation of peptidyl arginine deiminase (PAD) expression and an associated increase in the levels of citrullinated proteins are found in the synovium of patients with rheumatoid arthritis (79). Bioinformatic analysis has shown that *P. gingivalis* possesses a form of PAD that shares major sequence and structural homology with the *F. alocis* arginine deiminase enzyme (our unpublished data). Arginine deiminase of the pathogens was shown to possess multiple regulatory roles and was also shown to possess PAD function (80).

Our present study has shown the putative ability of the specific factors from *F. alocis* to modulate multiple changes in the host cell proteome (Fig. 7). It is likely that such variations at the molecular level are responsible for the functional changes required to mediate the pathogenic process. The relative resistance of *F. alocis* to oxidative stress (23) and its enhanced virulence potential in association with *P. gingivalis* collectively suggest its importance as a periodontal pathogen. The relative significance of specific *F. alocis* putative virulence factors that may trigger the key host response and hence the pathology awaits further clarification in the laboratory.

ACKNOWLEDGMENTS

This work was supported by Loma Linda University and Public Health Services grants DE13664, DE019730, DE019730 04S1, DE022508, and DE022724 from NIDCR (to H.F.).

REFERENCES

1. **Genco RJ, Van Dyke TE.** 2010. Prevention: reducing the risk of CVD in patients with periodontitis. Nat. Rev. Cardiol. **7:**479–480. http://dx.doi.org/10.1038/nrcardio.2010.120.
2. **Astolphi RD, Curbete MM, Colombo NH, Shirakashi DJ, Chiba FY, Prieto AK, Cintra LT, Bomfim SR, Ervolino E, Sumida DH.** 2013. Periapical lesions decrease insulin signal and cause insulin resistance. J. Endod. **39:**648–652. http://dx.doi.org/10.1016/j.joen.2012.12.031.
3. **Kaur S, White S, Bartold PM.** 2013. Periodontal disease and rheumatoid arthritis: a systematic review. J. Dent. Res. **92:**399–408. http://dx.doi.org/10.1177/0022034513483142.
4. **Bingham CO, Moni M.** 2013. Periodontal disease and rheumatoid arthritis: the evidence accumulates for complex pathobiologic interactions. Curr. Opin. Rheumatol. **25:**345–353. http://dx.doi.org/10.1097/BOR.0b013e32835fb8ec.
5. **Lamont RJ, Jenkinson HF.** 1998. Life below the gum line: pathogenic mechanisms of *Porphyromonas gingivalis*. Microbiol. Mol. Biol. Rev. **62:**1244–1263.
6. **Rudney JD, Chen R, Sedgewick GJ.** 2001. Intracellular *Actinobacillus actinomycetemcomitans* and *Porphyromonas gingivalis* in buccal epithelial cells collected from human subjects. Infect. Immun. **69:**2700–2707. http://dx.doi.org/10.1128/IAI.69.4.2700-2707.2001.
7. **Saito A, Inagaki S, Kimizuka R, Okuda K, Hosaka Y, Nakagawa T, Ishihara K.** 2008. *Fusobacterium nucleatum* enhances invasion of human gingival epithelial and aortic endothelial cells by *Porphyromonas gingivalis*. FEMS Immunol. Med. Microbiol. **54:**349–355. http://dx.doi.org/10.1111/j.1574-695X.2008.00481.x.
8. **Saito A, Inagaki S, Ishihara K.** 2009. Differential ability of periodontopathic bacteria to modulate invasion of human gingival epithelial cells by *Porphyromonas gingivalis*. Microb. Pathog. **47:**329–333. http://dx.doi.org/10.1016/j.micpath.2009.09.012.
9. **Dewhirst FE, Chen T, Izard J, Paster BJ, Tanner AC, Yu WH, Lakshmanan A, Wade WG.** 2010. The human oral microbiome. J. Bacteriol. **192:**5002–5017. http://dx.doi.org/10.1128/JB.00542-10.
10. **Liu B, Faller LL, Klitgord N, Mazumdar V, Ghodsi M, Sommer DD, Gibbons TR, Treangen TJ, Chang YC, Li S, Stine OC, Hasturk H, Kasif S, Segre D, Pop M, Amar S.** 2012. Deep sequencing of the oral microbiome reveals signatures of periodontal disease. PLoS One **7:**e37919. http://dx.doi.org/10.1371/journal.pone.0037919.
11. **Berezow AB, Darveau RP.** 2011. Microbial shift and periodontitis. Periodontol. 2000 **55:**36–47. http://dx.doi.org/10.1111/j.1600-0757.2010.00350.x.
12. **Griffen AL, Beall CJ, Campbell JH, Firestone ND, Kumar PS, Yang ZK, Podar M, Leys EJ.** 2012. Distinct and complex bacterial profiles in human periodontitis and health revealed by 16S pyrosequencing. ISME J. **6:**1176–1185. http://dx.doi.org/10.1038/ismej.2011.191.
13. **Gross EL, Leys EJ, Gasparovich SR, Firestone ND, Schwartzbaum JA, Janies DA, Asnani K, Griffen AL.** 2010. Bacterial 16S sequence analysis of severe caries in young permanent teeth. J. Clin. Microbiol. **48:**4121–4128. http://dx.doi.org/10.1128/JCM.01232-10.
14. **Paster BJ, Boches SK, Galvin JL, Ericson RE, Lau CN, Levanos VA, Sahasrabudhe A, Dewhirst FE.** 2001. Bacterial diversity in human subgingival plaque. J. Bacteriol. **183:**3770–3783. http://dx.doi.org/10.1128/JB.183.12.3770-3783.2001.
15. **Dahlén G, Leonhardt A.** 2006. A new checkerboard panel for testing bacterial markers in periodontal disease. Oral Microbiol. Immunol. **21:**6–11. http://dx.doi.org/10.1111/j.1399-302X.2005.00243.x.
16. **Kumar PS, Griffen AL, Barton JA, Paster BJ, Moeschberger ML, Leys EJ.** 2003. New bacterial species associated with chronic periodontitis. J. Dent. Res. **82:**338–344. http://dx.doi.org/10.1177/154405910308200503.
17. **Kumar PS, Leys EJ, Bryk JM, Martinez FJ, Moeschberger ML, Griffen AL.** 2006. Changes in periodontal health status are associated with bacterial community shifts as assessed by quantitative 16S cloning and sequencing. J. Clin. Microbiol. **44:**3665–3673. http://dx.doi.org/10.1128/JCM.00317-06.
18. **Leonhardt A, Carlen A, Bengtsson L, Dahlen G.** 2011. Detection of periodontal markers in chronic periodontitis. Open Dent. J. **5:**110–115. http://dx.doi.org/10.2174/1874210601105010110.
19. **Schlafer S, Riep B, Griffen AL, Petrich A, Hübner J, Berning M, Friedmann A, Göbel UB, Moter A.** 2010. *Filifactor alocis*—involvement in periodontal biofilms. BMC Microbiol. **10:**66. http://dx.doi.org/10.1186/1471-2180-10-66.
20. **Wade WG.** 2011. Has the use of molecular methods for the characterization of the human oral microbiome changed our understanding of the role of bacteria in the pathogenesis of periodontal disease? J. Clin. Periodontol. **38**(Suppl 11)**:**7–16. http://dx.doi.org/10.1111/j.1600-051X.2010.01679.x.
21. **Cato EP, Moore LVH, Moore WEC.** 1985. *Fusobacterium alocis* sp. nov. and *Fusobacterium sulci* sp. nov. from the human gingival sulcus. Int. J. Syst. Bacteriol. **35:**475–477. http://dx.doi.org/10.1099/00207713-35-4-475.
22. **Jalava J, Eerola E.** 1999. Phylogenetic analysis of *Fusobacterium alocis* and *Fusobacterium sulci* based on 16S rRNA gene sequences: proposal of *Filifactor alocis* (Cato, Moore and Moore) comb. nov. and *Eubacterium sulci* (Cato, Moore and Moore) comb. nov. Int. J. Syst. Bacteriol. **49**(Pt 4)**:**1375–1379. http://dx.doi.org/10.1099/00207713-49-4-1375.
23. **Aruni AW, Roy F, Fletcher HM.** 2011. *Filifactor alocis* has virulence attributes that can enhance its persistence under oxidative stress conditions and mediate invasion of epithelial cells by *Porphyromonas gingivalis*. Infect. Immun. **79:**3872–3886. http://dx.doi.org/10.1128/IAI.05631-11.
24. **Moffatt CE, Whitmore SE, Griffen AL, Leys EJ, Lamont RJ.** 2011. *Filifactor alocis* interactions with gingivalis epitheial cells. Mol. Oral Microbiol. **26:**365–373. http://dx.doi.org/10.1111/j.2041-1014.2011.00624.x.
25. **Wang Q, Jotwani R, Le J, Krauss JL, Potempa J, Coventry SC, Uriarte SM, Lamont RJ.** 30 December 2013. *Filifactor alocis* infection and inflammatory responses in the mouse subcutaneous chamber model. Infect. Immun. http://dx.doi.org/10.1128/IAI.01434-13.
26. **Wang Q, Wright CJ, Dingming H, Uriarte SM, Lamont RJ.** 2013. Oral community interactions of *Filifactor alocis* in vitro. PLoS One **8:**e76271. http://dx.doi.org/10.1371/journal.pone.0076271.
27. **Suzuki N, Yoneda M, Hirofuji T.** 6 March 2013. Mixed red-complex bacterial infection in periodontitis. Int. J. Dent. **2013:**587279. http://dx.doi.org/10.1155/2013/587279.
28. **Sharma S, Kelly TK, Jones PA.** 2010. Epigenetics in cancer. Carcinogenesis **31:**27–36. http://dx.doi.org/10.1093/carcin/bgp220.

29. **Rivenbark AG, Strahl BD.** 2007. Molecular biology. Unlocking cell fate. Science **318:**403–404. http://dx.doi.org/10.1126/science.1150321.
30. **Guo LH, Wang HL, Liu XD, Duan J.** 2008. Identification of protein differences between two clinical isolates of *Streptococcus mutans* by proteomic analysis. Oral Microbiol. Immunol. **23:**105–111. http://dx.doi.org/10.1111/j.1399-302X.2007.00394.x.
31. **Wilkins JC, Homer KA, Beighton D.** 2001. Altered protein expression of *Streptococcus oralis* cultured at low pH revealed by two-dimensional gel electrophoresis. Appl. Environ. Microbiol. **67:**3396–3405. http://dx.doi.org/10.1128/AEM.67.8.3396-3405.2001.
32. **Al-Haroni M, Skaug N, Bakken V, Cash P.** 2008. Proteomic analysis of ampicillin-resistant oral *Fusobacterium nucleatum*. Oral Microbiol. Immunol. **23:**36–42. http://dx.doi.org/10.1111/j.1399-302X.2007.00387.x.
33. **Xia Q, Wang T, Park Y, Lamont RJ, Hackett M.** 2007. Differential quantitative proteomics of *Porphyromonas gingivalis* by linear ion trap mass spectrometry: non-label methods comparison, q-values and LOWESS curve fitting. Int. J. Mass Spectrom. **259:**105–116. http://dx.doi.org/10.1016/j.ijms.2006.08.004.
34. **Xia Q, Wang T, Taub F, Park Y, Capestany CA, Lamont RJ, Hackett M.** 2007. Quantitative proteomics of intracellular *Porphyromonas gingivalis*. Proteomics **7:**4323–4337. http://dx.doi.org/10.1002/pmic.200700543.
35. **Lamont RJ, Meila M, Xia Q, Hackett M.** 2006. Mass spectrometry-based proteomics and its application to studies of *Porphyromonas gingivalis* invasion and pathogenicity. Infect. Disord. Drug Targets **6:**311–325. http://dx.doi.org/10.2174/187152606778249935.
36. **Aruni AW, Roy F, Sandberg L, Fletcher HM.** 2012. Proteome variation among *Filifactor alocis* strains. Proteomics **12:**3343–3364. http://dx.doi.org/10.1002/pmic.201200211.
37. **Tamura K, Dudley J, Nei M, Kumar S.** 2007. MEGA4: Molecular Evolutionary Genetics Analysis (MEGA) software version 4.0. Mol. Biol. Evol. **24:**1596–1599. http://dx.doi.org/10.1093/molbev/msm092.
38. **Johnson LS, Eddy SR, Portugaly E.** 2010. Hidden Markov model speed heuristic and iterative HMM search procedure. BMC Bioinformatics **11:**431. http://dx.doi.org/10.1186/1471-2105-11-431.
39. **Kanehisa M, Goto S, Furumichi M, Tanabe M, Hirakawa M.** 2010. KEGG for representation and analysis of molecular networks involving diseases and drugs. Nucleic Acids Res. **38:**D355–D360. http://dx.doi.org/10.1093/nar/gkp896.
40. **Yilmaz O, Young PA, Lamont RJ, Kenny GE.** 2003. Gingival epithelial cell signalling and cytoskeletal responses to *Porphyromonas gingivalis* invasion. Microbiology **149:**2417–2426. http://dx.doi.org/10.1099/mic.0.26483-0.
41. **Castañeda-Roldán EI, Avelino-Flores F, Dall'Agnol M, Freer E, Cedillo L, Dornand J, Girón JA.** 2004. Adherence of Brucella to human epithelial cells and macrophages is mediated by sialic acid residues. Cell. Microbiol. **6:**435–445. http://dx.doi.org/10.1111/j.1462-5822.2004.00372.x.
42. **Harris JR.** 2007. Negative staining of thinly spread biological samples. Methods Mol. Biol. **369:**107–142. http://dx.doi.org/10.1007/978-1-59745-294-6_7.
43. **Massey BW.** 1953. Ultra-thin sectioning for electron microscopy. Stain Technol. **28:**19–26.
44. **Wyffels JT.** 2001. Principles and techniques of electron microscopy: biological applications, 4th edition, by M. A. Hayat. Microsc. Microanal. **7:**66.
45. **Xiong L, Darwanto A, Sharma S, Herring J, Hu S, Filippova M, Filippov V, Wang Y, Chen CS, Duerksen-Hughes PJ, Sowers LC, Zhang K.** 2011. Mass spectrometric studies on epigenetic interaction networks in cell differentiation. J. Biol. Chem. **286:**13657–13668. http://dx.doi.org/10.1074/jbc.M110.204800.
46. **Kersey PJ, Duarte J, Williams A, Karavidopoulou Y, Birney E, Apweiler R.** 2004. The International Protein Index: an integrated database for proteomics experiments. Proteomics **4:**1985–1988. http://dx.doi.org/10.1002/pmic.200300721.
47. **Kolenbrander PE, Andersen RN, Blehert DS, Egland PG, Foster JS, Palmer RJ, Jr.** 2002. Communication among oral bacteria. Microbiol. Mol. Biol. Rev. **66:**486–505. http://dx.doi.org/10.1128/MMBR.66.3.486-505.2002.
48. **Kolenbrander PE, Palmer RJ, Jr, Rickard AH, Jakubovics NS, Chalmers NI, Diaz PI.** 2006. Bacterial interactions and successions during plaque development. Periodontol. 2000 **42:**47–79. http://dx.doi.org/10.1111/j.1600-0757.2006.00187.x.
49. **Patti JM, Allen BL, McGavin MJ, Hook M.** 1994. MSCRAMM-mediated adherence of microorganisms to host tissues. Annu. Rev. Microbiol. **48:**585–617. http://dx.doi.org/10.1146/annurev.mi.48.100194.003101.
50. **Fenno JC.** 21 February 2012. *Treponema denticola* interactions with host proteins. J. Oral Microbiol. http://dx.doi.org/10.3402/jom.v4i0.9929.
51. **Pinkston KL, Gao P, Diaz-Garcia D, Sillanpaa J, Nallapareddy SR, Murray BE, Harvey BR.** 2011. The Fsr quorum-sensing system of *Enterococcus faecalis* modulates surface display of the collagen-binding MSCRAMM Ace through regulation of gelE. J. Bacteriol. **193:**4317–4325. http://dx.doi.org/10.1128/JB.05026-11.
52. **Zhulin IB, Nikolskaya AN, Galperin MY.** 2003. Common extracellular sensory domains in transmembrane receptors for diverse signal transduction pathways in bacteria and archaea. J. Bacteriol. **185:**285–294. http://dx.doi.org/10.1128/JB.185.1.285-294.2003.
53. **Mougel C, Zhulin IB.** 2001. CHASE: an extracellular sensing domain common to transmembrane receptors from prokaryotes, lower eukaryotes and plants. Trends Biochem. Sci. **26:**582–584. http://dx.doi.org/10.1016/S0968-0004(01)01969-7.
54. **Jorth P, Whiteley M.** 2012. An evolutionary link between natural transformation and CRISPR adaptive immunity. mBio **3:**e00309-12. http://dx.doi.org/10.1128/mBio.00309-12.
55. **Cady KC, O'Toole GA.** 2011. Non-identity-mediated CRISPR-bacteriophage interaction mediated via the Csy and Cas3 proteins. J. Bacteriol. **193:**3433–3445. http://dx.doi.org/10.1128/JB.01411-10.
56. **Marraffini LA, Sontheimer EJ.** 2008. CRISPR interference limits horizontal gene transfer in staphylococci by targeting DNA. Science **322:**1843–1845. http://dx.doi.org/10.1126/science.1165771.
57. **Díez-Villaseñor C, Almendros C, García-Martínez J, Mojica FJ.** 2010. Diversity of CRISPR loci in *Escherichia coli*. Microbiology **156**(Pt 5)**:**1351–1361. http://dx.doi.org/10.1099/mic.0.036046-0.
58. **Watanabe T, Nozawa T, Aikawa C, Amano A, Maruyama F, Nakagawa I.** 2013. CRISPR regulation of intraspecies diversification by limiting IS transposition and intercellular recombination. Genome Biol. Evol. **5:**1099–1114. http://dx.doi.org/10.1093/gbe/evt075.
59. **Yin L, Chung WO.** 2011. Epigenetic regulation of human beta-defensin 2 and CC chemokine ligand 20 expression in gingival epithelial cells in response to oral bacteria. Mucosal Immunol. **4:**409–419. http://dx.doi.org/10.1038/mi.2010.83.
60. **Pathak SK, Basu S, Bhattacharyya A, Pathak S, Banerjee A, Basu J, Kundu M.** 2006. TLR4-dependent NF-kappaB activation and mitogen- and stress-activated protein kinase 1-triggered phosphorylation events are central to *Helicobacter pylori* peptidyl prolyl cis-, trans-isomerase (HP0175)-mediated induction of IL-6 release from macrophages. J. Immunol. **177:**7950–7958. http://dx.doi.org/10.4049/jimmunol.177.11.7950.
61. **Díaz-Jullien C, Pérez-Estévez A, Covelo G, Freire M.** 1996. Prothymosin alpha binds histones in vitro and shows activity in nucleosome assembly assay. Biochim. Biophys. Acta **1296:**219–227. http://dx.doi.org/10.1016/0167-4838(96)00072-6.
62. **Martic G, Karetsou Z, Kefala K, Politou AS, Clapier CR, Straub T, Papamarcaki T.** 2005. Parathymosin affects the binding of linker histone H1 to nucleosomes and remodels chromatin structure. J. Biol. Chem. **280:**16143–16150. http://dx.doi.org/10.1074/jbc.M410175200.
63. **Gomez-Marquez J, Rodriguez P.** 1998. Prothymosin alpha is a chromatin-remodelling protein in mammalian cells. Biochem. J. **333**(Pt 1)**:**1–3.
64. **Ushijima T, Hattori N.** 2012. Molecular pathways: involvement of *Helicobacter pylori*-triggered inflammation in the formation of an epigenetic field defect, and its usefulness as cancer risk and exposure markers. Clin. Cancer Res. **18:**923–929. http://dx.doi.org/10.1158/1078-0432.CCR-11-2011.
65. **Champion MD.** 2011. Host-pathogen o-methyltransferase similarity and its specific presence in highly virulent strains of *Francisella tularensis* suggests molecular mimicry. PLoS One **6:**e20295. http://dx.doi.org/10.1371/journal.pone.0020295.
66. **Wang Y, Curry HM, Zwilling BS, Lafuse WP.** 2005. Mycobacteria inhibition of IFN-gamma induced HLA-DR gene expression by up-regulating histone deacetylation at the promoter region in human THP-1 monocytic cells. J. Immunol. **174:**5687–5694. http://dx.doi.org/10.4049/jimmunol.174.9.5687.
67. **Seveau S, Bierne H, Giroux S, Prevost MC, Cossart P.** 2004. Role of lipid rafts in E-cadherin– and HGF-R/Met–mediated entry of *Listeria monocytogenes* into host cells. J. Cell Biol. **166:**743–753. http://dx.doi.org/10.1083/jcb.200406078.
68. **Lafont F, Abrami L, van der Goot FG.** 2004. Bacterial subversion of lipid rafts. Curr. Opin. Microbiol. **7:**4–10. http://dx.doi.org/10.1016/j.mib.2003.12.007.
69. **Wang M, Hajishengallis G.** 2008. Lipid raft-dependent uptake, signalling

and intracellular fate of *Porphyromonas gingivalis* in mouse macrophages. Cell Microbiol. **10:**2029–2042. http://dx.doi.org/10.1111/j.1462-5822.2008.01185.x.

70. **Knodler LA, Vallance BA, Hensel M, Jackel D, Finlay BB, Steele-Mortimer O.** 2003. Salmonella type III effectors PipB and PipB2 are targeted to detergent-resistant microdomains on internal host cell membranes. Mol. Microbiol. **49:**685–704. http://dx.doi.org/10.1046/j.1365-2958.2003.03598.x.
71. **Ezzell RM, Goldmann WH, Wang N, Parashurama N, Ingber DE.** 1997. Vinculin promotes cell spreading by mechanically coupling integrins to the cytoskeleton. Exp. Cell Res. **231:**14–26. http://dx.doi.org/10.1006/excr.1996.3451.
72. **Gautrey HL, Tyson-Capper AJ.** 2012. Regulation of Mcl-1 by SRSF1 and SRSF5 in cancer cells. PLoS One **7:**e51497. http://dx.doi.org/10.1371/journal.pone.0051497.
73. **Mayran N, Parton RG, Gruenberg J.** 2003. Annexin II regulates multivesicular endosome biogenesis in the degradation pathway of animal cells. EMBO J. **22:**3242–3253. http://dx.doi.org/10.1093/emboj/cdg321.
74. **Andrés V, González JM.** 2009. Role of A-type lamins in signaling, transcription, and chromatin organization. J. Cell Biol. **187:**945–957. http://dx.doi.org/10.1083/jcb.200904124.
75. **Thuny F, Textoris J, Amara AB, Filali AE, Capo C, Habib G, Raoult D, Mege JL.** 2012. The gene expression analysis of blood reveals S100A11 and AQP9 as potential biomarkers of infective endocarditis. PLoS One **7:**e31490. http://dx.doi.org/10.1371/journal.pone.0031490.
76. **Seemann J, Weber K, Gerke V.** 1997. Annexin I targets S100C to early endosomes. FEBS Lett. **413:**185–190. http://dx.doi.org/10.1016/S0014-5793(97)00911-3.
77. **He H, Li J, Weng S, Li M, Yu Y.** 2009. S100A11: diverse function and pathology corresponding to different target proteins. Cell Biochem. Biophys. **55:**117–126. http://dx.doi.org/10.1007/s12013-009-9061-8.
78. **Eisenreich W, Heesemann J, Rudel T, Goebel W.** 2013. Metabolic host responses to infection by intracellular bacterial pathogens. Front. Cell Infect. Microbiol. **3:**24. http://dx.doi.org/10.3389/fcimb.2013.00024.
79. **Foulquier C, Sebbag M, Clavel C, Chapuy-Regaud S, Al Badine R, Méchin MC, Vincent C, Nachat R, Yamada M, Takahara H, Simon M, Guerrin M, Serre G.** 2007. Peptidyl arginine deiminase type 2 (PAD-2) and PAD-4 but not PAD-1, PAD-3, and PAD-6 are expressed in rheumatoid arthritis synovium in close association with tissue inflammation. Arthritis Rheum. **56:**3541–3553. http://dx.doi.org/10.1002/art.22983.
80. **Touz MC, Ropolo AS, Rivero MR, Vranych CV, Conrad JT, Svard SG, Nash TE.** 2008. Arginine deiminase has multiple regulatory roles in the biology of *Giardia lamblia*. J. Cell Sci. **121:**2930–2938. http://dx.doi.org/10.1242/jcs.026963.